iScience, Volume *23*

Supplemental Information

Spermidine Suppresses Inflammatory DC Function by Activating the FOXO3 Pathway and Counteracts Autoimmunity

Guanhua Li, Huihua Ding, Xiang Yu, Yao Meng, Jun Li, Qiang Guo, Haibo Zhou, and Nan Shen

Transparent Methods

Mice

All mouse studies were approved by the Animal Care Committee of Renji Hospital. The C57BL/6J and BALB/c mice were purchased from Slack Company. *Foxo3a*$^{-/-}$ mice were generated via CRISPR/Cas9 system. Briefly, sgRNAs-targeting the introns on both sides of the exon 2 of *Foxo3a* were respectively constructed and transcribed in vitro. Then Cas9 mRNA and sgRNA will be co-injected into zygotes. Thereafter, the zygotes were transferred into the oviduct of pseudo pregnant ICR females at 0.5 dpc. And F0 mice was birthed after 19~21 days of transplantation. All the off springs of ICR females (F0 mice) were examined by PCR and sequencing of tail DNA. Finally, positive F0 mice were crossed with C57BL/6J mice to build up heterozygous mice. Mice were bred and housed under SPF conditions. All mice were male at 8-10 weeks of age.

Metabolomics

MoDCs were incubated in the presence or absence of IFN-α. After 24 hours, cells were collected to perform extraction of metabolites. IFN-DC were incubated with R837 (InvivoGen), in presence of absence of spermidine (Sigma-Aldrich). After 0.5, 4 and 16 hours, samples were collected to perform extraction of metabolites. Amino acids were measured in cell samples that were previously stored at −80°C using a quantitative UPLC-MS/MS platform (ACQUITY UPLC-Xevo TQ-S, Waters Corp., Milford, MA, USA) according to previously published methods (Chen et al., 2016a; Chen et al., 2016b). All chromatographic separations were performed with an ACQUITY BEH C18 column VanGuard pre-column (2.1×5 mm) and analytical column (2.1×100 mm). The elution solvents were water with 0.2% formic acid (A) and acetonitrile with 0.2% formic acid (B). The flow rate was 500μl/min with the following mobile phase gradient: 0–0.38 min (1% B), 0.38–3 min (1–15% B), 3–5.4 min (15–70% B), 5.5–5.9 min (100% B), and 5.9–6.6 min (100-1% B). The cone and collision energy for each amino acid used the optimized settings from QuanOptimize application manager. All of the amino acid standards were obtained from Sigma-Aldrich (St. Louis, MO, USA), and 14 stable isotope- labeled standards were obtained from Cambridge Isotope Laboratories, Inc. (Tewksbury, MA, USA). The standards and stable isotope-labeled standards were accurately weighed and prepared in water to obtain individual stock solution at a concentration of 5.0 or 20.0 mM. The stock solution of individual amino acids was mixed and prepared to obtain a series of amino acid calibrators at a final concentration of 5000, 2500, 500, 150, 10, 2.5, or 1 nM. The raw data generated by UPLC-MS/MS were then processed using the QuanMET software (v1.0, Metabo-Profile, Shanghai, China) to perform peak integration, calibration, and quantitation for each amino acid.

IMQ-induced Psoriasis-like Mouse Model and Spermidine Treatment

Male BALB/c mice (6–8 weeks of age) were induced by a daily topical dose of IMQ cream (5%) on the shaved back for 6 consecutive days, and then sacrificed for H&E staining. Control mice were treated with the same dose of vehicle cream. Redness, scaling were scored independently on a scale from 0 to 4: 0, none; 1, slight; 2, moderate;

3, marked; 4, very marked. Male BALB/c mice were intraperitoneally injected with spermidine (40mg/kg weight) on day 0, 1, 2 and 3 during the application of IMQ.

Cell Isolation, Flow Cytometry Analysis, and Cell Sorting.

Skin cells were prepared according to previous studies with minor modification (Cai et al., 2011). Briefly, the epidermis and dermis were separated from the skin using dispase (Roche) (25U/ml in 1640), and the epidermal cells was prepared by trypsin (Gibco) digestion, and the dermal cells by collagenase (Sigma-Aldrich) and hyaluronidase (Sigma-Aldrich) digestion. Cells were analyzed using Fortessa (BD) and FlowJo (v10.0.7). Splenocytes were separated by digesting the tissue fragments with collagenase IV (Sigma-Aldrich) and DNase I (Sigma-Aldrich). Antibodies used for cell staining were listed in Table S1. Data were analyzed using Fortessa (BD) and FlowJo (v10.0.7).

Cells were cultured in RPMI 1640 medium (Gibco) with 10% fetal bovine serum (FBS, Gibco) and 1% Penicillin-Streptomycin (Gibco) at 37°C and 5% CO_2 or collected directly for subsequent experiments. To obtain moDCs, mouse monocytes were isolated from BM with the Mouse Monocyte Isolation Kit (BM) according to the technical manual (Miltenyi, Germany). Cells were cultured with 100ng/mL GM-CSF (Peprotech) and 50ng/mL IL-4 (Peprotech) for 7 days and then sorted by Flow cytometry (FACSAriaTM III, BD). IFN-DC were obtained by pre-stimulating moDC with 2000U/mL mouse IFN-α (PBL) for 24 hours. Then, IFN-DC were stimulated with 10μg/mL R837 (Invivogen) for 24 hours. MoDC were stimulated with 1μg/mL LPS (Invivogen) or 5mM ODN2216 (Invivogen) for 24 hours.

ECAR and OCR Measurement

MoDCs were pretreated with or without IFN-α overnight. IFN-DC were incubated with R837 (InvivoGen) in presence or absence of spermidine overnight. Then cells were seeded into XF96-well plates (Agilent) at $2x10^5$ cells per well in 3-6 duplicates. For ECAR test, seahorse base media was supplemented with 2mM glutamine. For the mito-stress OCR test, base media was supplemented with 2mM glutamine (Sigma-Aldrich), 2mM sodium pyruvate (Sigma-Aldrich) and 10mM glucose (Sigma-Aldrich). Plates were incubated in a CO_2 free incubator at 37°C for 1 h and then transfer to the seahorse machine for detection. Measurements were made using an XFe96 Analyzer (Agilent) and results were processed with Wave 2.6.0 software.

Hematoxylin and Eosin Staining

Mouse skin tissues were fixed in formalin and embedded in paraffin. Sections were stained with hematoxylin and eosin. Epidermal hyperplasia was assessed by measuring the thickness of the epidermis from the basal layer to the stratum corneum using Case Viewer software (3DHISTECH Ltd). The epidermal thickness was measured on 10 randomly selected areas per x10 field from three to five fields per skin. All the measurements were performed blinded to the treatment groups. The results were first averaged per mouse and then averaged per treatment group for statistical analysis.

Depletion of Monocytes and Neutrophils

The depletion was performed as previously described. Briefly, to deplete monocytes and neutrophils, the mice were injected intraperitoneally with 500mg/mice/day of anti-Gr1 (clone RB6-8C5, BioXCell, West Lebanon, NH, USA) on days 0, 1, 2, 3 and 4. To deplete neutrophils alone, the mice were injected intraperitoneally with 500mg/mice/day anti-Ly6G (clone 1A8, BioXCell, West Lebanon, NH, USA) using the same schedule.

MRNA-sequencing

Total RNA was extracted by Trizol reagent (Invitrogen) and determined by Bioanalyzer 4200 (Agilent, Santa Clara, CA, USA). Then, the next-generation libraries of mRNA were prepared using VAHTS mRNA-seq v2 Library Prep Kit for Illumina® (Vazyme, Nanjing, China). The Library quality was determined by Bioanalyzer 4200 (Agilent, Santa Clara, CA, USA). Then the mRNA-seq libraries were sequenced in HiSeq x10 system (Illumina, San Diego, CA, USA) on a 150bp paired-end run. The differentially expressed genes were selected as having more than 1 fold difference in their geometrical mean expression between the compared groups and a statistically significant p-value (<0.05) by analysis of DEseq2. The GO analysis on differentially expressed genes was performed with an R package: Clusterprofiler using a $p<0.05$ to define statistically enriched GO categories. Pathway analysis was used to determine the significant pathway of the differential genes according to Kyoto Encyclopedia of Genes and Genomes Database (http://www.genome.jp/kegg/) and DAVID Bioinformatics Resources 6.8 (https://david.ncifcrf.gov/).

Quantitative Real-time RT–PCR

Total RNA of moDCs and IFN-DCs was extracted by Trizol reagent (Invitrogen). The extraction of RNA from whole skins were performed using RNeasy Fibrous Tissue Mini Kit (Qiagen, Hilden, Germany) according to the manufacturer's instructions. cDNA was prepared by reverse transcription (PrimeScript RT Reagent kit; Takara) and amplified by real-time quantitative PCR (qPCR) with the primers shown in Table S2. Amplification was performed in an ABI PRISM 7900 Real Time PCR System (Applied Biosystems). The amplification efficiency of these genes was the same as that for *β-actin*, as indicated by the standard curves for amplification. The expression of mRNAs were normalized to *β-actin* mRNA by calculating $2^{-\Delta Ct}$, where Ct is the cycle threshold.

Immunoblots

2×10^6 DCs were lysed in radioimmune precipitation assay lysis and extraction buffer (Thermo Fisher Scientific). Nuclear and cytoplasmic extracts were prepared using a NE-PER Nuclear and Cytoplasmic Extraction Kit (Thermo Fisher Scientific). Individual cell lysates (10μg/lane) were separated by 10% SDS-PAGE and transferred to an Immobilon-P polyvinylidene difluoride membrane (Millipore, Billerica, MA). After being blocked with SuperBlock T20 PBS blocking buffer (Thermo Fisher Scientific, Pittsburgh, PA), the membranes were incubated with antibodies listed in the

Table S1.

Cytokine Detection

Serum from IMQ induced mice were collected on indicated time points, and cytokines were detected by BD™ Cytometric Bead Array (CBA) Mouse Flex Sets. Mouse serum IFN-α was detected by Mouse IFN α ELISA Kit (PBL, 42120-1). Cell supernatant was collected and analyzed by ELISA kit according to manufacturer's instructions for IL-6 (Biolegend, 431307), TNF-α (Biolegend, 430907), and IL-12/IL-23 p40 (Thermo Fisher, 88-7120-22).

Statistics

For all experiments, data were analyzed by two-tailed unpaired *t* test or one-way ANOVA. The data were analyzed by Graph Prism 7.0 software (GraphPad Software Inc.), p values were provided as * $p < 0.05$, ** $p < 0.01$, *** $p < 0.001$, n.s. not significant.

Data and Software Availability

RNA seqencing transcriptomic data are deposited in the Gene Expression Omnibus repository (GSE142452).

References

Cai, Y., Shen, X., Ding, C., Qi, C., Li, K., Li, X., Jala, V.R., Zhang, H.G., Wang, T., Zheng, J., et al. (2011). Pivotal role of dermal IL-17-producing gammadelta T cells in skin inflammation. Immunity 35, 596-610.

Chen, T., Ni, Y., Ma, X., Bao, Y., Liu, J., Huang, F., Hu, C., Xie, G., Zhao, A., Jia, W., et al. (2016a). Branched-chain and aromatic amino acid profiles and diabetes risk in Chinese populations. Sci Rep 6, 20594.

Chen, T., Zheng, X., Ma, X., Bao, Y., Ni, Y., Hu, C., Rajani, C., Huang, F., Zhao, A., Jia, W., et al. (2016b). Tryptophan Predicts the Risk for Future Type 2 Diabetes. PLoS One 11, e0162192.

Supplemental Figure legends

Figure S1. Sorting strategy of moDCs, Related to Figure 1. (A) MoDCs were sorted as $FV575^{-}CD11c^{+}MHCII^{hi}CD11b^{int}$ cells. FV575, live/die dye. FSC-A, FSC-W, SSC-A and SSC-W were used to gate single cells. (B, left) The expression of F4/80 in moDCs and macrophage. (B, right) The morphology of sorted moDCs and macrophages. (C) The purity of sorted moDCs. All the data are representative of three independent experiments.

Figure S2. Spermidine do not affect the apoptosis of IFN-DCs, Related to Figure 2. (A) BM monocytes were cultured with GM-CSF and IL-4 for 7 days. MoDCs were sorted and treated with 2000U/mL IFN-α for 24 hours. Then, IFN-DCs were stimulated with R837, together with or without 15μM spermidine for 24 hours. The survival of IFN-DC was detected by using flow cytometry. Live cells, $FV575^{-}$ cells. Data are representative of three independent experiments. (B) Sorted moDCs were stimulated with IFN-α alone or IFN-α plus SPD overnight. The relative mRNA levels of *TLR7* are shown (n=3). (C) TLR7 transfected moDCs were pretreated with or without 1 mM DFMO, and then stimulated with R837 for 24 hours. The expression of TNF-α and IL-6 are shown (n=3). (D) MoDCs were primed with IFN-α or IFN-α plus SPD, and then stimulated with R837 for 24 hours. The expression of TNF-α and IL-6 are shown (n=3). (E) MoDCs were stimulated with 1μg/mL LPS or 5μM ODN2216 together with or without 30μM SPD for 24 hours. The protein levels of TNF-α and IL-6 are shown (n=3). All data are representative of two independent experiments and shown as mean ±SEM. p values were determined by two-tailed unpaired t test *p<0.05, **p<0.01, ***p<0.001.

Figure S3. Spermidine inhibits autoimmune related pathways, Related to Figure 4. IFN-DCs were cultured with R837, together with or without spermidine for 18 hours. Cells were collected and the mRNA expression was detected by RNA-seq. Changed genes enriched pathways were shown.

Figure S4. FOXO3 partially mediates the anti-inflammatory effect of Spermidine, Related to Figure 4. (A) The ratios of phosphorylated protein to total protein at 0min time point were set as 1, respectively. (B) The ratios of phosphorylated protein to total protein at 0min time point of SPD group were set as 1, respectively. Data are representative of three independent experiments and shown as mean ±SEM. p values were determined by two-tailed unpaired *t* test *p<0.05, **p<0.01, ***p<0.001. The difference at 30min time point in (B) were statistically analyzed. (C) BM cells were isolated from WT or *Foxo3a*$^{-/-}$ mice, and the expression of FOXO3 was detected by immunoblot. Data are representative of two independent experiments.

Figure S5. IMQ induces the expression of IFN-α and TLR7 while spermidine hampers the induction, Related to Figure 5. (A) Mice were painted with IMQ on the back and ear. 8 hours later, the expression of IFN-α in serum were detected. (B) The expression of *TLR7* mRNA in the dermal moDCs isolated from IMQ induced mice at

indicated time points. (C) The expression of *TLR7* mRNA in the dermal moDCs isolated from IMQ induced mice with or without spermidine treatment on day 4. The expression of mRNAs were normalized to *β-actin* mRNA by calculating $2^{-\Delta Ct}$ (n=5). Data are representative of two independent experiments and shown as mean ±SEM. p values were determined by two-tailed unpaired *t* test. *p<0.05, **p<0.01, ***p<0.001, n.s. not significant.

Figure S6. Administration of spermidine ameliorates the systematic inflammation of IMQ-induced psoriasis-like mice, Related to Figure 5. Mice were treated with IMQ and spermidine as the schedule shown in Figure 5A. (A) Pictures and weight of spleen (n=5-7). (B) Gating strategy of splenocytes. (C) The number of splenic $Ly6c^{hi}$ monocytes, macrophages, neutrophils, B cells, pDCs, $CD8\alpha^+$ cDCs, $CD8\alpha^-$ cDCs, $CD4^+$ T cells and $CD8^+$ T cells (n=5). Data are representative of two independent experiments and shown as mean ±SEM. p values compare the indicated groups using a two-tailed unpaired Student's *t* test. *p<0.05, **p<0.01, n.s. not significant.

Figure S7. Spermidine inhibits the infiltration of moDCs and activation of γδT cells, Related to Figure 5. (A) Flow cytometry analysis of moDC or (B) $IL\text{-}17A^+$ γδT in the dermal skin from IMQ induced mice with or without spermidine treatment.

Figure S8. IFN-DC participates in the anti-psoriasis process of spermidine, Related to Figure 6. (A) The depletion efficiency of anti-Gr1 and anti-Ly6G antibody in vivo. (B) The number of macrophages, neutrophils, B cells, pDCs, $CD8\alpha^+$ cDCs, $CD8\alpha^-$ cDCs, $CD4^+$ T cells and $CD8^+$ T cells from the spleen of indicated mice in Figure 6 (n=5). Data are representative of two independent experiments and shown as mean ±SEM. p values were determined by two-tailed unpaired *t* test. *p<0.05, **p<0.01, ***p<0.001, n.s. not significant.

Supplemental Tables

Table S1. Antibody list used in the paper, Related to Figure 2-6.
Table S2. Primer list used in the paper, Related to Figure 1 and 5.

Figure S1

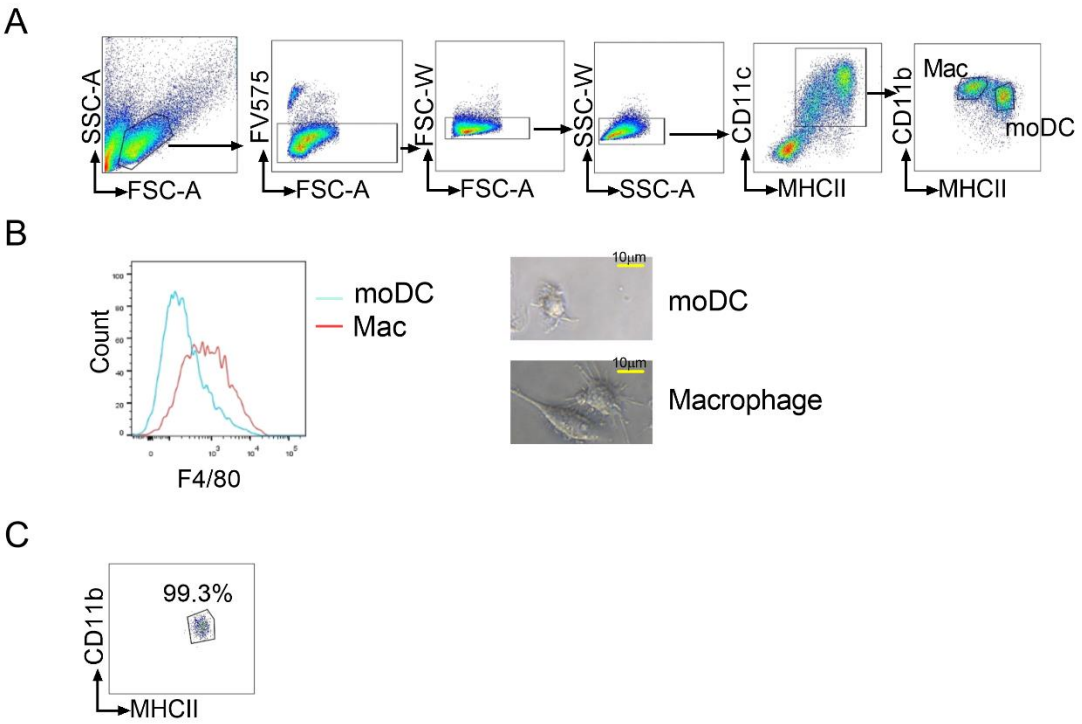
A
SSC-A
FSC-A
FV575
FSC-A
FSC-W
FSC-A
SSC-W
SSC-A
CD11c
MHCII
CD11b
MHCII
Mac
moDC
B
Count
F4/80
moDC
Mac
10μm
moDC
10μm
Macrophage
C
CD11b
MHCII
99.3%

Figure S2

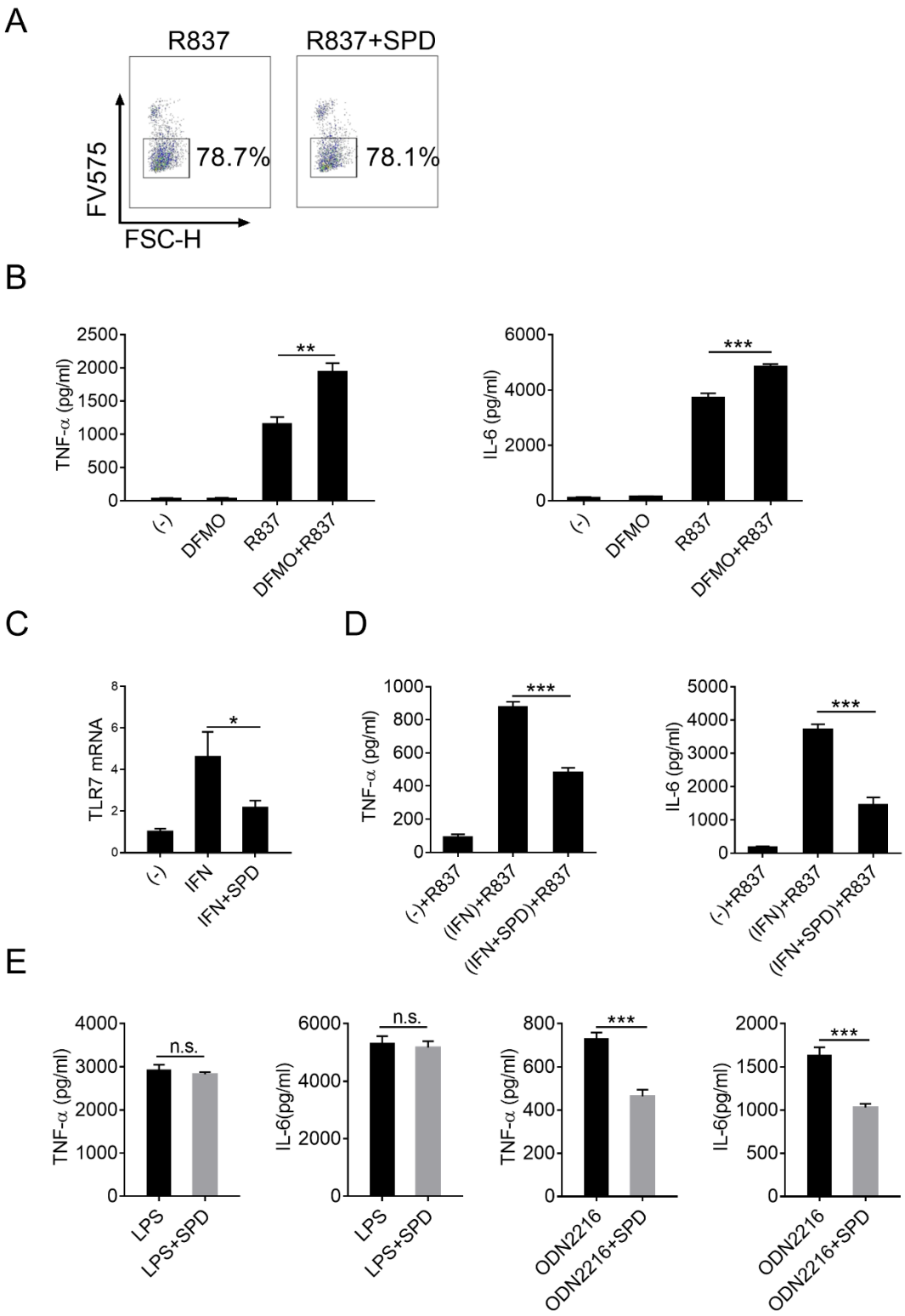
A
R837
R837+SPD
78.7%
78.1%
FV575
FSC-H
B
TNF-α (pg/ml)
IL-6 (pg/ml)
(-)
DFMO
R837
DFMO+R837
C
TLR7 mRNA
IFN
IFN+SPD
D
(-)+R837
(IFN)+R837
(IFN+SPD)+R837
E
n.s.
LPS
LPS+SPD
IL-6(pg/ml)
ODN2216
ODN2216+SPD

Figure S3

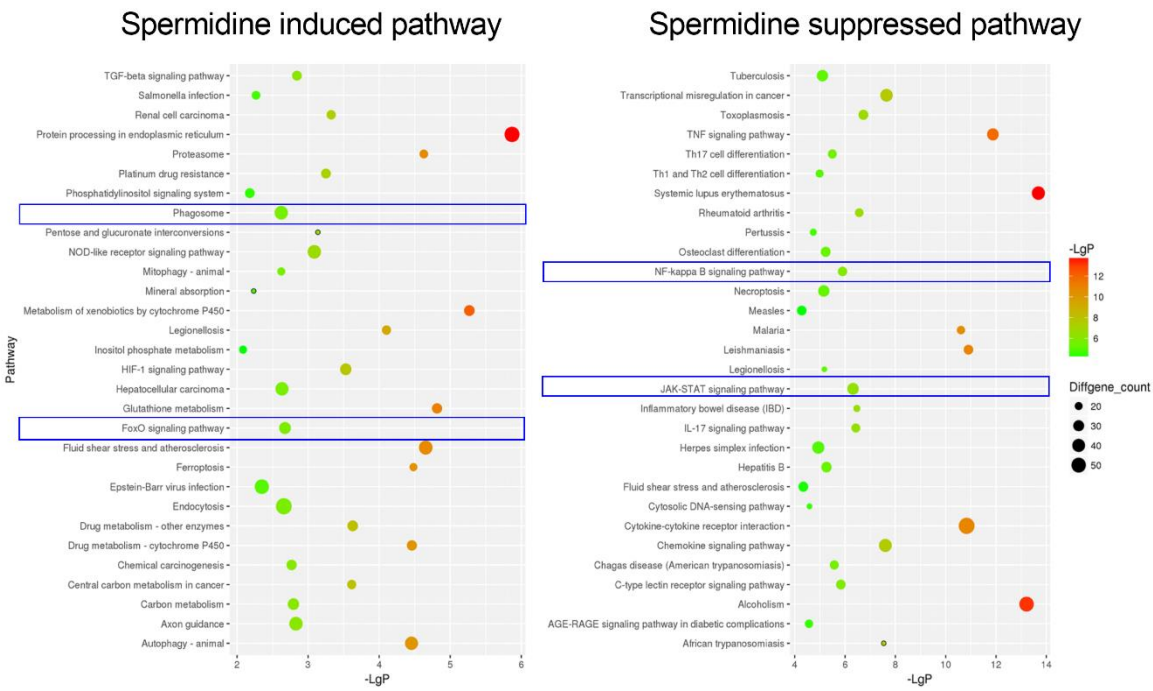
Spermidine induced pathway
Spermidine suppressed pathway
TGF-beta signaling pathway
Salmonella infection
Renal cell carcinoma
Protein processing in endoplasmic reticulum
Proteasome
Platinum drug resistance
Phosphatidylinositol signaling system
Phagosome
Pentose and glucuronate interconversions
NOD-like receptor signaling pathway
Mitophagy - animal
Mineral absorption
Metabolism of xenobiotics by cytochrome P450
Legionellosis
Inositol phosphate metabolism
HIF-1 signaling pathway
Hepatocellular carcinoma
Glutathione metabolism
FoxO signaling pathway
Fluid shear stress and atherosclerosis
Ferroptosis
Epstein-Barr virus infection
Endocytosis
Drug metabolism - other enzymes
Drug metabolism - cytochrome P450
Chemical carcinogenesis
Central carbon metabolism in cancer
Carbon metabolism
Axon guidance
Autophagy - animal
Pathway
2
3
4
5
6
-LgP
Tuberculosis
Transcriptional misregulation in cancer
Toxoplasmosis
TNF signaling pathway
Th17 cell differentiation
Th1 and Th2 cell differentiation
Systemic lupus erythematosus
Rheumatoid arthritis
Pertussis
Osteoclast differentiation
NF-kappa B signaling pathway
Necroptosis
Measles
Malaria
Leishmaniasis
Legionellosis
JAK-STAT signaling pathway
Inflammatory bowel disease (IBD)
IL-17 signaling pathway
Herpes simplex infection
Hepatitis B
Fluid shear stress and atherosclerosis
Cytosolic DNA-sensing pathway
Cytokine-cytokine receptor interaction
Chemokine signaling pathway
Chagas disease (American trypanosomiasis)
C-type lectin receptor signaling pathway
Alcoholism
AGE-RAGE signaling pathway in diabetic complications
African trypanosomiasis
4
6
8
10
12
14
-LgP
-LgP
12
10
8
6
Diffgene_count
20
30
40
50

Figure S4

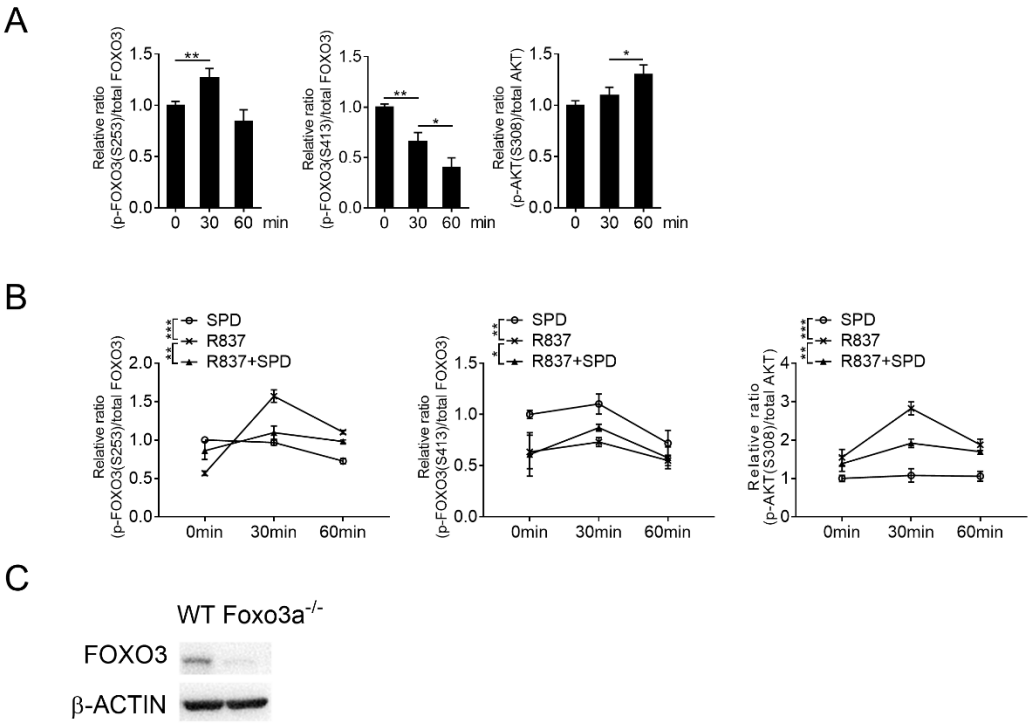
A
Relative ratio (p-FOXO3(S253)/total FOXO3)
Relative ratio (p-FOXO3(S413)/total FOXO3)
Relative ratio (p-AKT(S308)/total AKT)
0 30 60 min
B
SPD
R837
R837+SPD
Relative ratio (p-FOXO3(S253)/total FOXO3)
Relative ratio (p-FOXO3(S413)/total FOXO3)
Relative ratio (p-AKT(S308)/total AKT)
0min 30min 60min
C
WT Foxo3a-/-
FOXO3
β-ACTIN

Figure S5

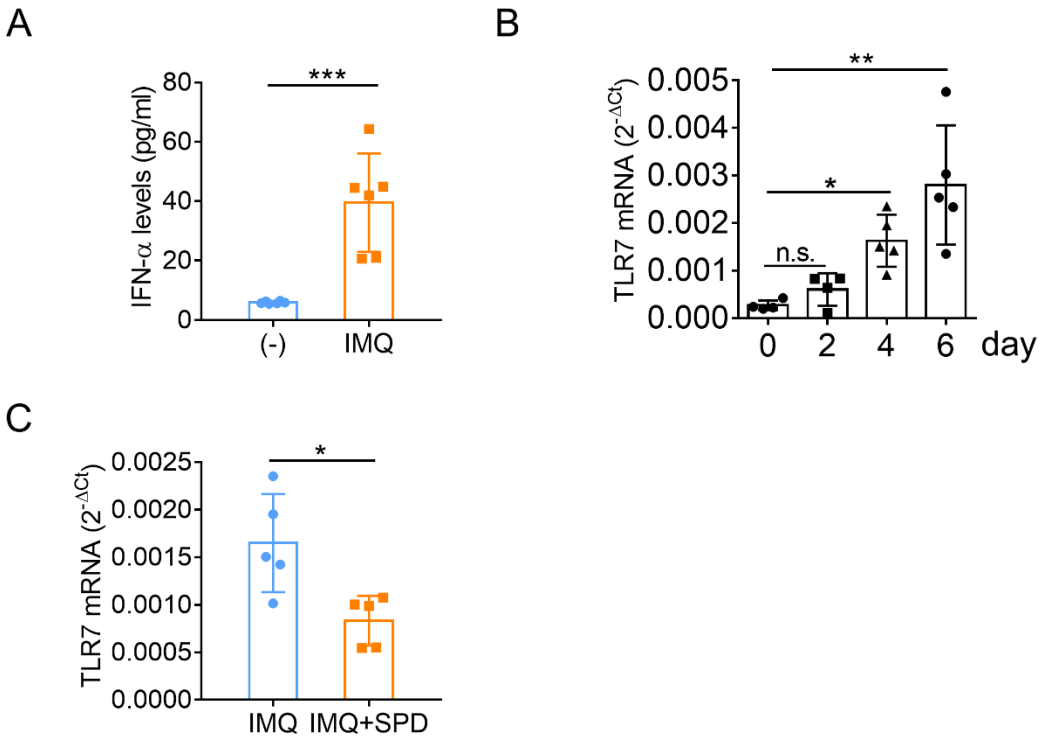
A
IFN-α levels (pg/ml)
80
60
40
20
0
***
(-)
IMQ
B
TLR7 mRNA (2^-ΔCt)
0.005
0.004
0.003
0.002
0.001
0.000
**
*
n.s.
0
2
4
6
day
C
TLR7 mRNA (2^-ΔCt)
0.0025
0.0020
0.0015
0.0010
0.0005
0.0000
*
IMQ
IMQ+SPD

Figure S6

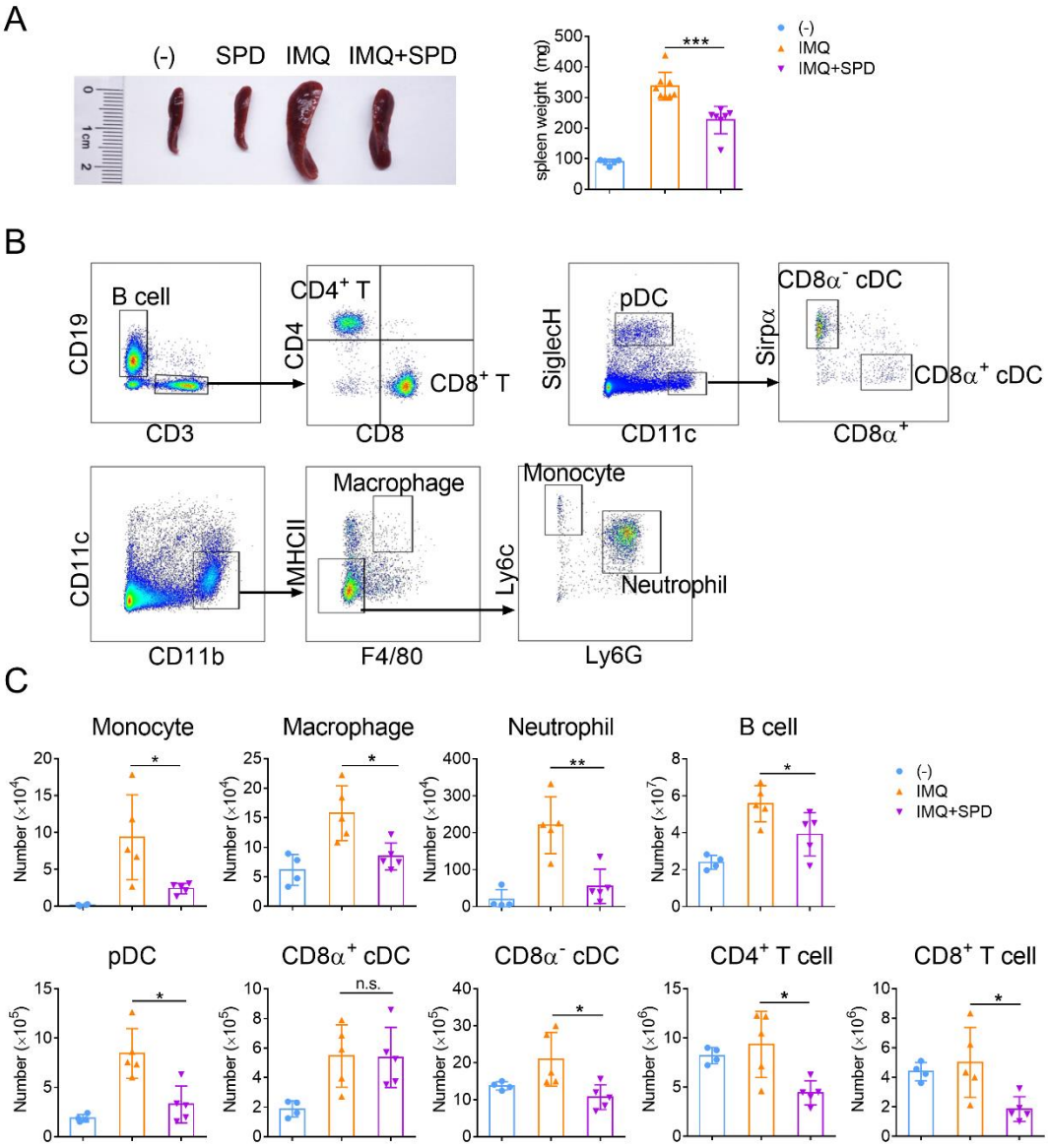
A
(-)
SPD
IMQ
IMQ+SPD
spleen weight (mg)
***
B
B cell
CD19
CD3
CD4⁺ T
CD4
CD8⁺ T
CD8
pDC
SiglecH
CD11c
CD8α⁻ cDC
Sirpα
CD8α⁺ cDC
CD8α⁺
CD11c
CD11b
Macrophage
MHCII
F4/80
Monocyte
Ly6c
Neutrophil
Ly6G
C
Monocyte
Macrophage
Neutrophil
B cell
pDC
CD8α⁺ cDC
CD8α⁻ cDC
CD4⁺ T cell
CD8⁺ T cell
Number (×10⁴)
Number (×10⁷)
Number (×10⁵)
Number (×10⁶)
n.s.
(-)
IMQ
IMQ+SPD

Figure S7

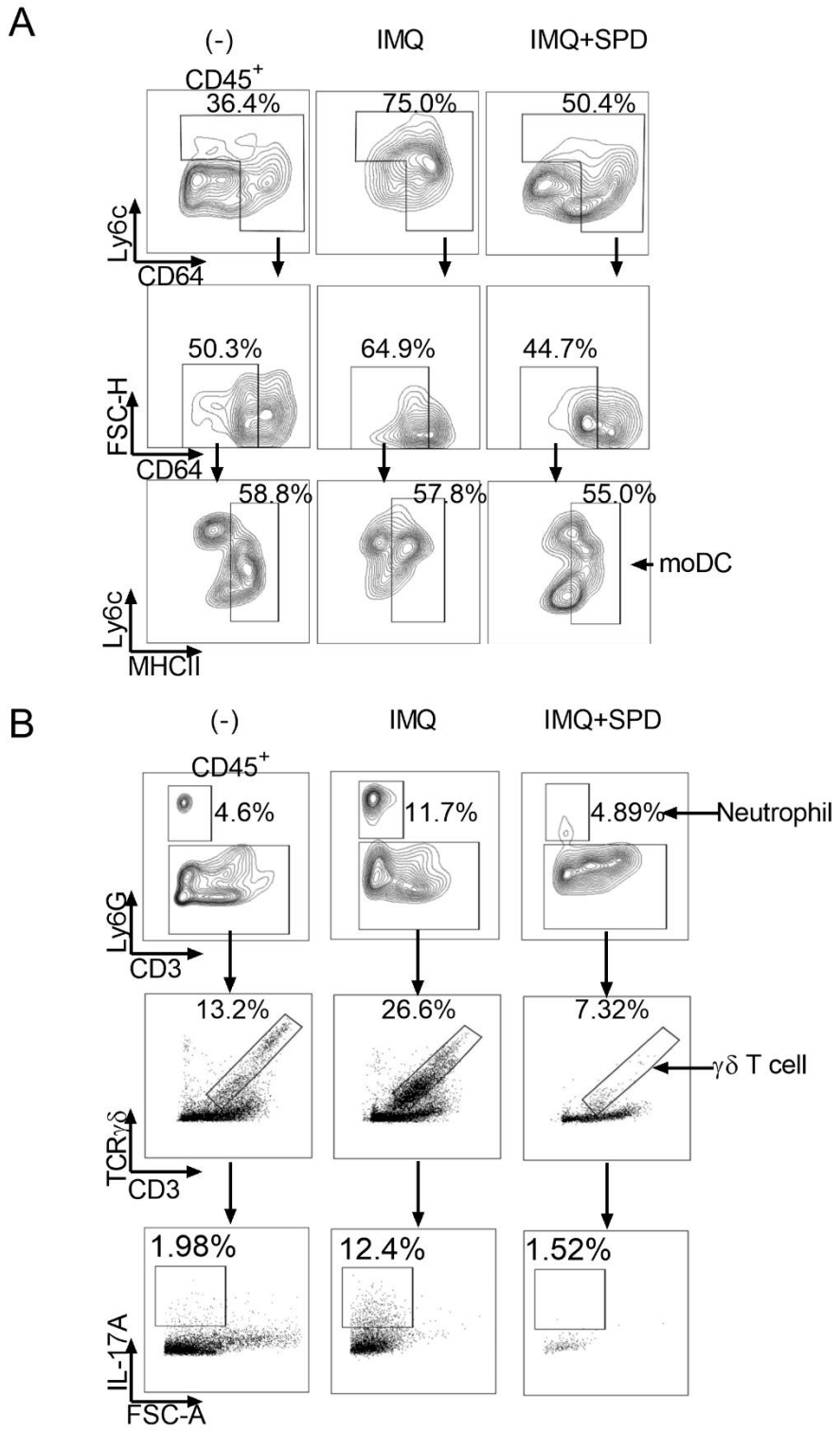
A
(-)
IMQ
IMQ+SPD
CD45+
36.4%
75.0%
50.4%
Ly6c
CD64
50.3%
64.9%
44.7%
FSC-H
CD64
58.8%
57.8%
55.0%
moDC
Ly6c
MHCII
B
(-)
IMQ
IMQ+SPD
CD45+
4.6%
11.7%
4.89%
Neutrophil
Ly6G
CD3
13.2%
26.6%
7.32%
γδ T cell
TCRγδ
CD3
1.98%
12.4%
1.52%
IL-17A
FSC-A

Figure S8

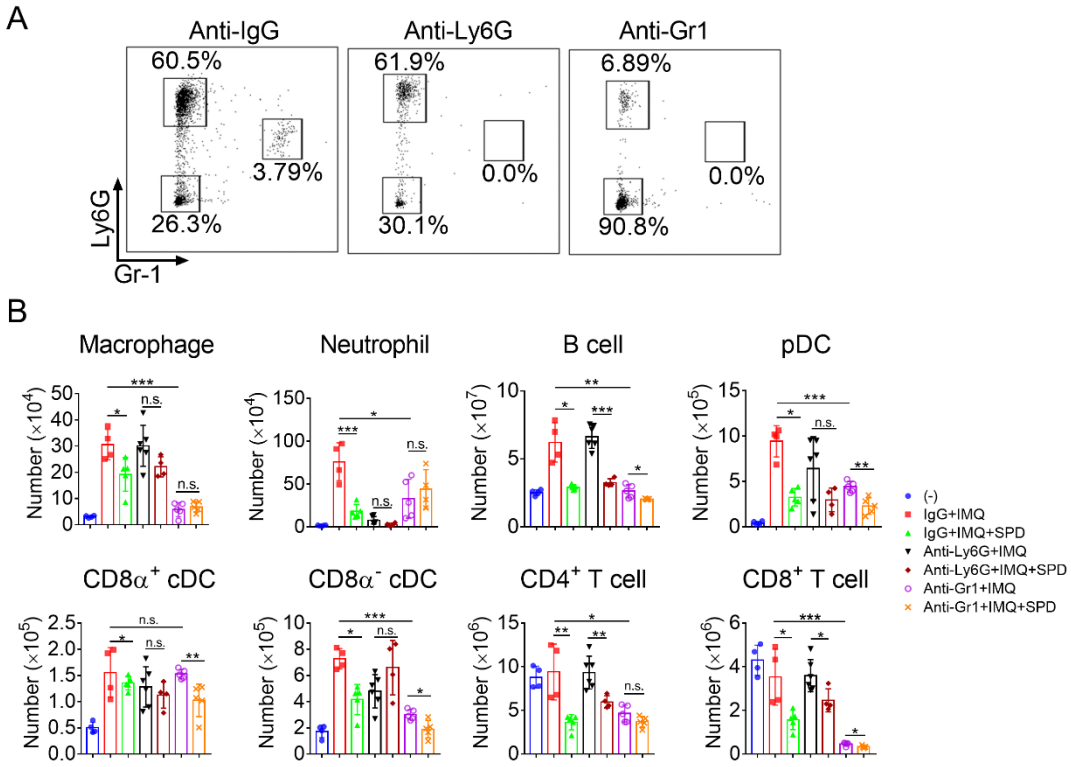
A
Anti-IgG
Anti-Ly6G
Anti-Gr1
60.5%
3.79%
26.3%
61.9%
0.0%
30.1%
6.89%
0.0%
90.8%
Ly6G
Gr-1
B
Macrophage
Neutrophil
B cell
pDC
CD8α+ cDC
CD8α- cDC
CD4+ T cell
CD8+ T cell
Number (×10^4)
Number (×10^7)
Number (×10^5)
Number (×10^6)
n.s.
(-)
IgG+IMQ
IgG+IMQ+SPD
Anti-Ly6G+IMQ
Anti-Ly6G+IMQ+SPD
Anti-Gr1+IMQ
Anti-Gr1+IMQ+SPD

Table S1

Antibodies	Source	Cat#
Anti-mouse CD45 - APC-CY7	BioLegend	103116
Anti-mouse CD3 - PE-CY7	BioLegend	100220
Anti-mouse CD4 - FITC	BioLegend	100406
Anti-mouse TCR γδ - APC	BioLegend	118116
Anti-mouse Ly6G - Percp-cy5.5	BioLegend	127616
Anti-mouse MHC Ⅱ - BV510	BioLegend	107636
Anti-mouse CD64 - PE	BioLegend	139304
Anti-mouse Ly6C - FITC	BioLegend	128006
Anti-mouse CD11b - PE-CY7	BioLegend	101216
Anti-mouse CD11c - Percp-cy5.5	BioLegend	117328
Anti-mouse CD103 - FITC	BioLegend	121420
Anti-mouse CD19 - BV510	BioLegend	115546
Anti-mouse CD11c - FITC	BioLegend	117306
Anti-mouse Ly6C - BV605	BioLegend	128036
Anti-mouse CD8α - PE-CY7	BioLegend	100722
Anti-mouse CD8α - Percp-cy5.5	BioLegend	100733
Anti-mouse IL17A - PE	BD	559502
Anti-mouse Siglec H – PE-CY7	Invitrogen	25-0333-82
Anti-mouse CD45 - APC	BioLegend	103112
Anti-mouse CD107a - APC	BioLegend	144014
Anti-mouse Ly6G - APC	BioLegend	127614
Anti-mouse CD3 - APC	BioLegend	100236
Anti-mouse Ly6G/Ly6C(Gr-1) - APC	BioLegend	108412
Anti-mouse CD40 - PE-CY7	BioLegend	124622
Anti-mouse CD86 - Percp-cy5.5	BioLegend	105028
Anti-mouse I-A/I-E- BV510	BioLegend	107641
NF-κB P65(D14E12)	CST	8242
Phospho-NF-κB P65 (Ser536) Antibody	CST	3033
β-Actin(13E5) Rabbit mAb	CST	4970
AMPKα (D5A2) Rabbit mAb	CST	5831
Phospho-AMPKα (Thr172) (40H9) Rabbit mAb	CST	2535
Phospho-4E-BP1 (Thr37/46) (236B4) Rabbit mAb	CST	2855
4E-BP1 (53H11) Rabbit mAb	CST	9644
Phospho-p70 S6 Kinase (Thr389) antibody	CST	9205
p70 S6 Kinase antibody	CST	9202
Phospho-Raptor (Ser792) antibody	CST	2083
Raptor (24C12) Rabbit mAb	CST	2280
Phospho-Akt (Ser473) Antibody	CST	9271
Akt antibody	CST	9272
Phospho-FoxO3a (Ser253) Antibody	CST	9466

Phospho-FoxO3a (Ser413) (D77C9) Rabbit mAb	CST	8174
FoxO3a (D19A7) Rabbit mAb	CST	12829
Anti-mouse IgG, HRP-linked antibody	CST	7076
Anti-rabbit IgG, HRP-linked antibody	CST	7074
Anti-mouse Ly6G	BioCell	1A8
Anti-mouse Ly6G/Gr1	BioCell	RB6-8C5
Lamin B1 Antibody	proteintech	66095-1-Ig

Table S2

species	gene	Forward(5'-3')	Reverse(5'-3')
mouse	*Arg1*	CATTGGCTTGCGAGACGTAGAC	GCTGAAGGTCTCTTCCATCACC
	Odc1	TGCCACACTCAAAACCAGCAGG	ACACTGCCTGAACGAAGGTCTC
	β-actin	GGCTGTATTCCCCTCCATCG	CCAGTTGGTAACAATGCCATGT
	Sms	GATGTACGCCAAAGAAGGGAGAG	CAGGTCGAGAATCAGTCTGAGG
	Srm	CGTTGGCTTCTCCAGCTCAAAG	AGGACTCCTTGAAGAGGCTCTC
	Ssat1	GAGGATGGCTTTGGAGAACACC	GATACAGCAACTTGCCAATCCATG
	Nos2	GAGACAGGGAAGTCTGAAGCAC	CCAGCAGTAGTTGCTCCTCTTC
	IL-17a	GAC TCT CCA CCG CAATGA	CTT CAG GAC CAG GAT CTC TT
	IL-23a	CAA CTC CTC CAG CCA GAG	GAA CCT GGG CAT CCT TAA
	IL-6	TGA AGT TCC TCT CTG CAA GA	GAA GTG GTA TAG ACA GGT CTG TT
	TNF-α	TCG GGT TGA GAA GAT CAT T	TAG ATT CCT GGA AGC ATA GAA